Advances in Science and Technology Research Journal

Advances in Science and Technology Research Journal 2024, 18(2), 214–225
https://doi.org/10.12913/22998624/184091
ISSN 2299-8624, License CC-BY 4.0

Received: 2023.12.18
Accepted: 2024.02.13
Published: 2024.03.14

Damages of the Section Insulator Guide Caused by Electric Arc

Jarosław Konieczny[1*], Krzysztof Labisz[1]

[1] Department of Railway Transport, Faculty of Transport and Aviation Engineering, Silesian University of Technology, ul. Krasińskiego 8, 40-019 Katowice, Poland

* Corresponding author's e-mail: jaroslaw.konieczny@polsl.pl

ABSTRACT

This article presents research on the influence of an electric arc on the properties and structure of a traction section guide made of ETP (electrolytic tough pitch) copper in a segment insulator of a railway section. An electrical discharge occurring during use, which may accompany the passage of the pantograph current collector between adjacent guides, may cause many physical phenomena. In addition to existing guide wear mechanisms, such as friction, corrosion, and/or oxidation, the action of an electric arc also has a devastating effect on the guide in use, causing its complete destruction in extreme cases. The aim of the investigation was to determine what type of damage to the sectional guide in real operation conditions was caused by the impact of an electric arc that is induced when the pantograph passes from one guide to the adjacent one. The paper presents the results of tests on an operational guide made of hard electrolytic copper Cu-ETP, in particular the results of microscopic observations, the results of microscopic tests obtained using the ZEISS SUPRA 25 scanning electron microscope, as well as the analysis of the chemical composition in micro-areas (EDS - Energy-dispersive X-ray spectroscopy). On the basis of the tests carried out, it was found that the dominant destructive mechanism of the guide is the electric arc, the presence of elements from the external environment was also determined, and the degree of damage was analysed depending on the conditions and operating times.

Keywords: electric arc discharge, copper, insulator guide, Cu-ETP, railway infrastructure

INTRODUCTION

Sectional insulator guides made of Cu-ETP copper are exposed to wear and damage caused by various mechanisms during operation. The first is frictional wear [1] of the graphite-made surface of the current collector, mounted on the pantograph, which is adjacent to the overhead contact line. According to the regulations of PKP PLK S.A. (Polskie Koleje Państwowe Polskie Linie Kolejowe – Polish State Railways Polish Railway Lines) [2], this current collector is now equipped with a graphite cap (Fig. 1).

Corrosion is another wear mechanism. Copper oxidation is associated with an increase in the intensity of this process due to the increase in temperature. As shown in work [3], copper oxidation occurs already at a temperature of 200 °C. The increase in temperature is associated with providing energy to oxygen and copper atoms, which then bind together more easily to form copper oxygen. Moreover, as the energy increases, the diffusion of oxygen atoms from the surrounding air occurs more easily and effectively into the copper. The increase in temperature is mainly caused by the flow of current, especially when high power is consumed when the train starts to come to a standstill. Another cause of the temperature increase at the interface between the guide and the graphite current collector is the phenomenon of friction [4, 5].

However, the most destructive mechanism is the electric arc, which arises during the passage of the pantograph through a section insulator (Fig. 2) and the physical phenomena generated with it [6], including local, short-term temperature increase up to a maximum of 20,000 °C [7], rapid expansion of evaporated metal and air [8], molten metal particles, shock and sonic waves [9]. Under the influence of increasing temperature, the guide material plasticises. This increases the possibility of deformation of the guide [6] because, in order to ensure its constant contact with the current collector, the pantograph is equipped with elements ensuring constant pressure and adherence to the working part (Figure 1). In addition, the rapid increase in the volume of the material as a result of its melting, as well as due to the shock wave, the molten particles of the Cu-ETP material are splashed around, which may cause damage or destruction of rolling stock elements, and is also dangerous for the infrastructure owner employees working there [10].

The tests were performed on used guides of section insulators, which were elements of railway traction. On the railway routes where the tested guides were installed, the trains reached a maximum speed of 120 km/h or 40 km/h (Fig. 2). They were replaced after 6 or 12 months and 12 months, respectively. In the case discussed in the article, the test samples presented in Figures 4 and 5 were tested after operation on a route where trains moved at a speed of up to 40 km/h (12 months of operation). However, the described case is not common and its occurrence is quite rare. The purpose of the research was to investigate and describe what type of damage to the sectional guide in real-life conditions is caused by an electric arc that is induced when the pantograph moves from one guide to the adjacent one.

MATERIALS AND METHODS

The section insulator guide was manufactured in accordance with the arrangements of PKP PLK S.A. [11] with Cu-ETP materials with the chemical composition shown in Table 1 (according to the standard [12, 13]).

The prepared samples were taken from the guides used and placed in phenolic resin for further preparation. After that the samples were ground on sandpaper with increasingly finer grains and polished with an Al_2O_3 suspension. In the next stage of polishing the metallographic samples, Al_2O_3 was replaced with a diamond suspension with a grain size of 1 μm. The samples were etched in a solution of: 2 g of potassium chromate $K_2Cr_2O_7$, 100 cm^3 of distilled water, 4 cm^3 of sodium chloride NaCl solution, 8 cm^3 of sulphuric acid H_2SO_4. The samples were alternately polished and etched to obtain the correct image of the microstructure. The microstructure of the tested material was observed using an Olympus light microscope and a Zeiss Supra scanning electron microscope (SEM). The chemical composition of the tested microareas was examined using the energy dispersive spectroscopy (EDS) method.

The X-ray phase analysis was performed using a Panalytical X'Pert X-ray diffractometer. Filtered radiation from a cobalt anode lamp was used. The measurement step was 0.05, and the pulse counting time was chosen at 10 s.

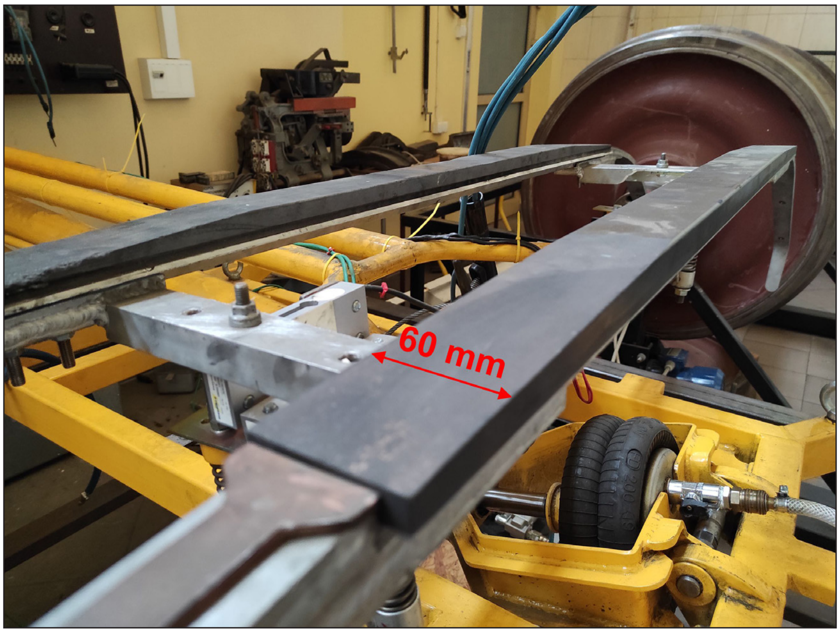

Fig. 1. A fragment of the current collector with a visible graphite cap

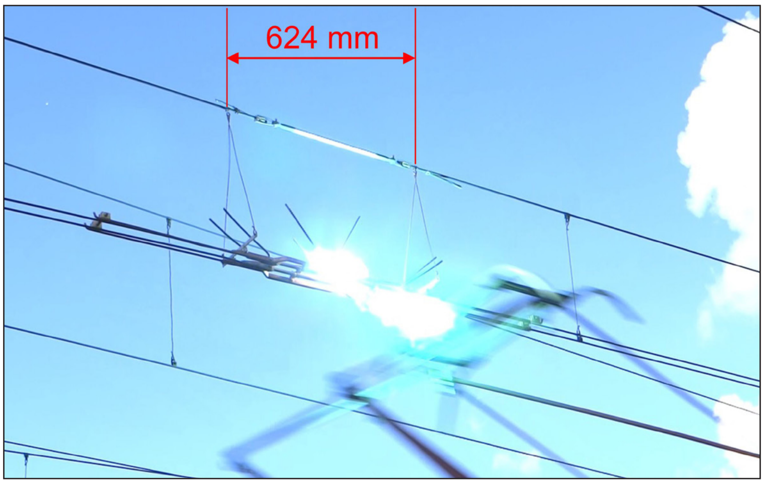

Fig. 2. Electric arc caused by the pantograph movement between the guides of the section insulator

Table 1. Chemical composition of Cu-ETP copper [12, 13]

Copper mark	Cu	Ag	O	Bi	Pb	Balance
Cu-ETP	99,9	0.015	0.04	0.0005	0.005	0.03 (bez Ag,O)

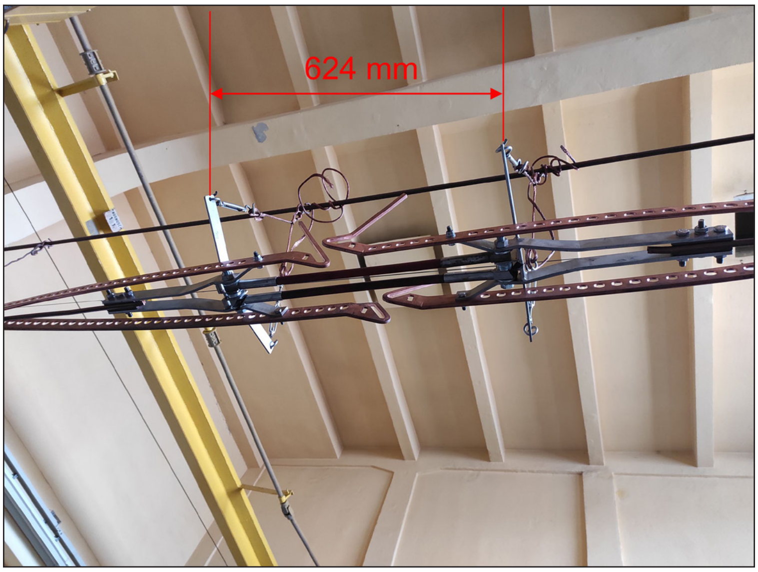

Fig. 3. Bottom view of the section insulator; placed outside, there are guides made of Cu-ETP copper

RESULTS

The phenomenon of electric arc discharge when the current collector jumps from one guide to another is accompanied by the generation of a very high temperature, which may cause melting of parts of the guide. This event may occur for various reasons. One of them may be wear of the guide, which does not extinguish the arc by changing the geometry of the blowing horns. Such events are rare, but they do occur, as the photo below shows (Figure 4). Numerous drops of solidified copper are visible on the guide. Figure 5 shows the working surface of the guide; it shows no signs of tribological wear, but burnt craters are clearly visible and there are drops of solid copper on the side surface. Visible changes in the guide surface are the result of the electric arc.

Figure 5 shows the impact of high temperature generated when an electric arc is discharged on the guide (working) surface of the guide. Microstructure observations made using a scanning electron microscope (SEM) showed the presence of molten copper drops. This is the result of the melting of copper due to the high temperature that is generated when a discharge occurs in the form of an electric arc. In this area, traces of melting of the guide material were also found on the surface (Fig. 6). Although the high temperature is short-lived, it has locally reached the copper melting point.

Figure 6 shows the working surface of the guide, which was the subject of the research. No traces of tribological wear were found. Grooves and burnt craters are clearly visible on the side surface, as well as drops of solidified copper resulting from spatter during the discharge of an electric arc. Additionally, quite numerous recesses and holes (holes and pits) are visible, which are also formed as a result of melting of the guide surface under the influence of an electric arc. Any changes occurring on the surface of the Cu-ETP copper guide are the result of electrical discharges during the operation of the traction network.

Another observed impact of electric arc discharge on the investigated copper guide made of Cu-ETP is the formation of cracks on its surface, as can be seen in Figure 7. The drawing shows the outer layer of the guide melt with burns and/or craters, as well as numerous traces of cracks occurring on this surface, similar to the impact of laser surface melting, carried out with HPDL laser for the purpose of enhancing the characteristic of the treated surface [36]. These cracks are most likely the result of relatively quick solidification of metal (Cu), which was previously melted at high temperature during the occurrence of electric arc discharges. Similar results were reported in the study reported in [14].

Moreover, based on the analysis of the scattered X-ray spectrum (EDS) performed on the surface of the guide exposed to the electric arc, the presence of elements occurring on the surface of the molten conductor and originating from the external environment was found, as well as a large amount of oxides (Table 2). What may be surprising is the relatively high content of chlorine, silicon, sulphur, carbon and iron, as well as minimal amounts of aluminium, phosphorus and potassium. These elements can also act as a factor influencing the hardening of the surface layer of the insulator guide, but they also reduce the electrical conductivity [37].

DISCUSSION

The effect of energy during the discharge of an electric arc influencing the degree of wear damage of the carbon strip was investigated in [15]. It was found that there is a proportional relationship between the degree of belt wear (W_s) and the electrical arc energy (E), which is linear (Fig. 8). Using the nonlinear least squares regression method, this relationship was determined by the Equation 1:

$$W_s = 0.65E + 0.379 \quad (1)$$

where: $R^2 = 0.79$.

Moreover, it was also found that the wear damage level of the belt surface in which thermal mechanisms dominate depends both on the intensity and acting time of the electric arc. The most often occurring wear mechanisms for the present carbon strip are evaporation erosion and

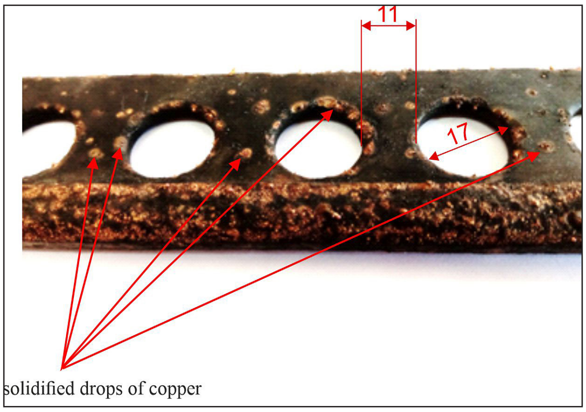

Fig. 4. Damaged section guide; macro observations; maximum train speed on the route was 40 km/h (replaced after 1 year)

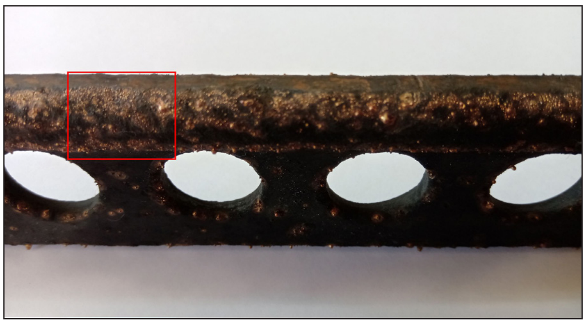

Fig. 5. The working (sliding) surface of the guide and the side surface with traces of the influence of an electric arc; macro observations; and the maximum train speed on the route was 40 km/h (replaced after 1 year)

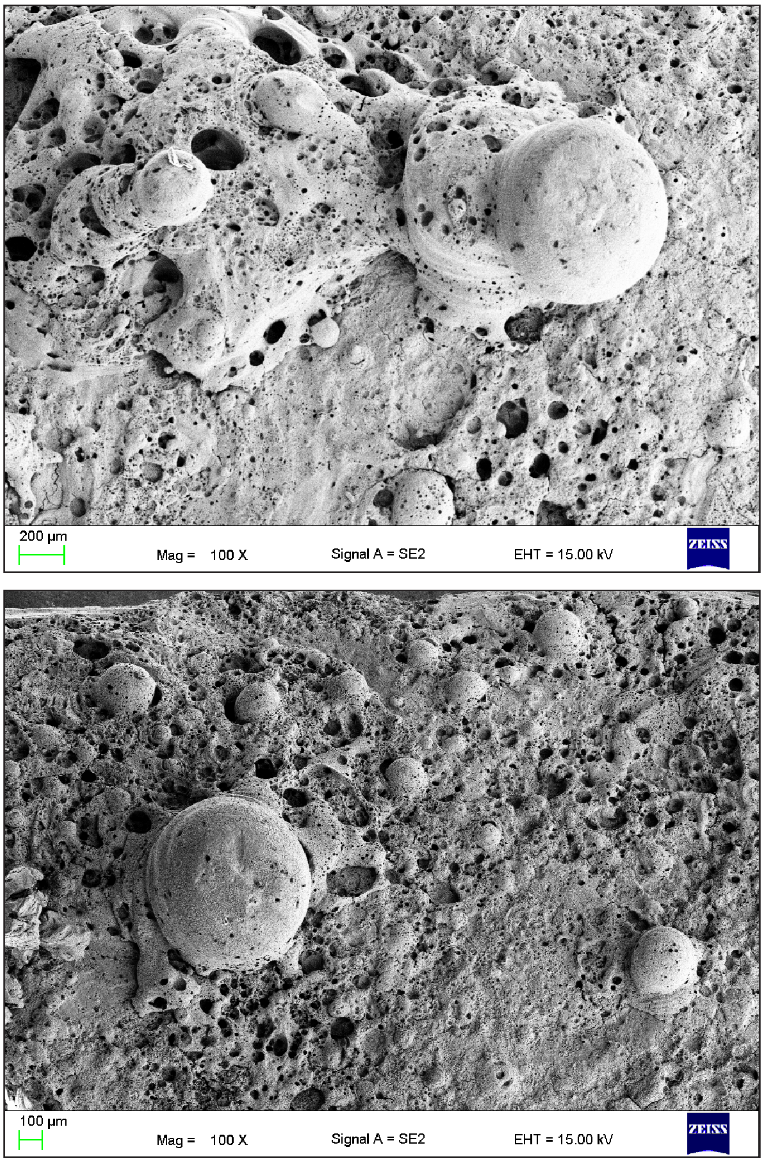

Fig. 6. (a) Working surface of the guide of a section insulator melted with an electric arc, view from the boxed area in Fig. 5; (b) the adjacent area to Fig. 6a, shown enlarged

material diffusion. The authors of this publication noticed a similar phenomenon of guide degradation (Fig. 4 and Fig. 5). An electric arc consists of many separate, simultaneous discharges. The typical spot size observed in the structure is in the sub-micrometre range; local melting may result in the formation of a large number of characteristic cavities and pits (Figs. 6 and 7). The arc emigrates from one place to another with a relatively high probability of igniting near the pits formed by previous arcs, which ultimately leads to the formation of visible traces on a macro scale, which consist of a large number of craters of several micrometres in size [16, 17]. Arc erosion that appears during the use of the connector also depends on the surface quality, among others: from the occurrence of dirt [17, 18]. The electric arc can move rapidly and ablate the top of the material and may also cause erosion on the surface. The phenomenon of erosion occurs as a result of the action of arc plasma, which occurs, among others, under the influence of high temperature, and the material of the surface layer melts or evaporates [19]. The melted material may only move by a few microns as a result of diffusion – this is how craters are created and the material is splashed under the influence of the pressure of the drops creating the plasma in the electric arc (Figs. 4 and 5) [20]. A large number of erosion pits and spent material particles were disclosed, as well as surface deposits resulting from material melting and high-temperature spattering (Fig. 7). In

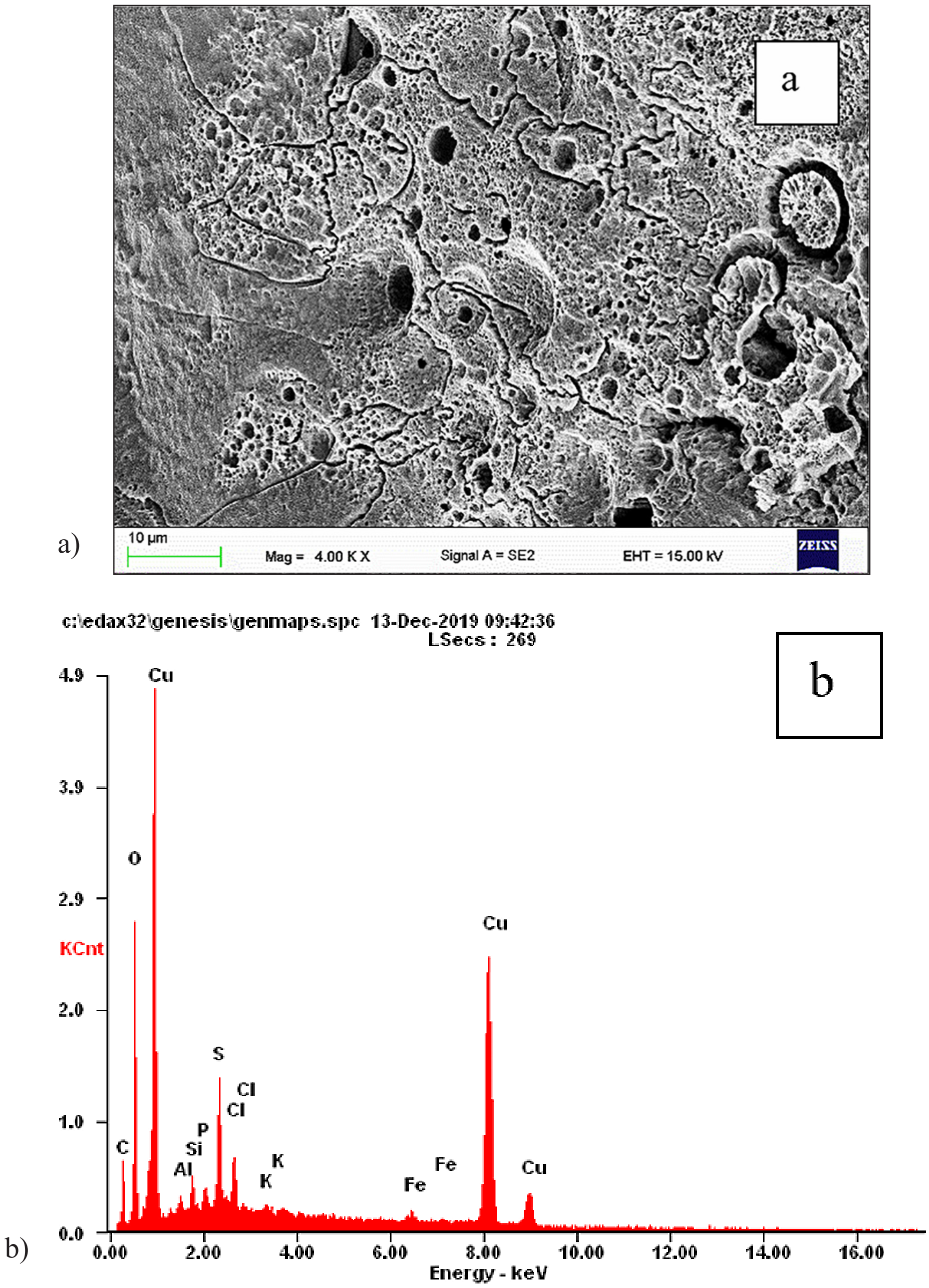

Fig. 7. (a) Guide surface deformed by an electric arc; (b) analysis of the chemical composition of the area shown in the Fig. 7a; SEM

[21] it was found that heavy arc erosion weakens the conductivity of the carbon strip, resulting in a decrease in the conductivity value of the applied carbon strip, and thus affects the quality of the current collection by the train. One of the most important factors influencing the formation of an electric arc during friction in the copper-graphite pair with a flowing electric current is the presence of load [22]. It should be noted that the arc energy increases with a decrease in stress and an increase in electric current. At lower values of normal loads ($F_n \leq 1.0$ N), during tests with an applied electric current, the friction process occurring is small and unstable. On the other hand, the friction coefficient is subject to quite high variability due to the occurrence of an electric arc at short intervals.

Additionally, the found investigation results revealed that the amount of carbon overlay wear is mostly influenced by the electric arc, which causes a significant increase in the volume of the used material, and the wear mechanisms consists mainly of the electric arc ablation and the additional tacking and material transfer. Of the other mechanisms, mechanical friction has the highest

Table 2. Results of the chemical composition analysis Fig. 7b

Element	Wt%	At%
CK	14.34	33.42
OK	19.04	33.30
AlK	0.76	0.79
SiK	1.15	1.14
PK	0.73	0.66
SK	3.93	3.43
ClK	1.84	1.45
KK	0.37	0.27
FeK	1.03	0.52
CuK	56.80	25.02

influence on wear; however, the volume of material used is disproportionately lower compared to the wear caused by the electric arc. The investigation results have revealed, similarly to the work [21], the effect of arc erosion that occurs on the surface of the investigated insulator guide part.

In the work [23, 24] were investigated the influence of the arc discharge was investigated on the wear rate of a copper-impregnated carbon tape that works together with a wire made of pure copper. The obtained test results confirmed that the very intense influence of this factor as well as the fact that the dominant wear mechanisms in this case are the thermal effects of the discharge on the strip surface: material melting, evaporation, loss of impregnated copper particles and carbon oxidation. Similar results were achieved in this work (Fig. 4 and Fig. 6). These mechanisms wear out the carbon belt material when sliding under the influence of electric current. The wear rate depends on the intensity that occurred and duration of the arc discharge. It is proportional to the arc energy, i.e. the product of the intensity and duration of the discharge.

Based on the results presented in [23], a graph of the wear rate of arc discharge energy was drawn, and then a straight line (function) was approximated to the line (Fig. 9), which is characterised by the equation presented below (2):

$$y = 1.2023x + 4.7413 \qquad (2)$$

Which is determined by the Pearson linear correlation coefficient: $R^2 = 0.7187$. The R^2 coefficient, called the coefficient of determination, determines the degree of fit of the determined function resulting from the approximation to the real data, so it can be interpreted as a measure of the fit of the developed model to the experimental data. With regard to the obtained results, it should be stated that Equation 1 obtained by approximating the results is almost 80% consistent with them and reliably determines the relationship between wear rate and electrical arc energy of the electric arc. Similarly, in the case of Equation 3, a quite high effect, 71%, of compliance of the experimental data with the proposed equation describing the relationship between strip wear rate and discharge energy was obtained.

The thermal wear as well as arc erosion and abrasive wear, are the dominant wear mechanisms that occur in the process of sliding friction with the coexisting electrical current flow accompanying material transfer [25].

The observed wear of the carbon strip through delamination occurs and propagates under conditions of strong erosive wear caused by an electric

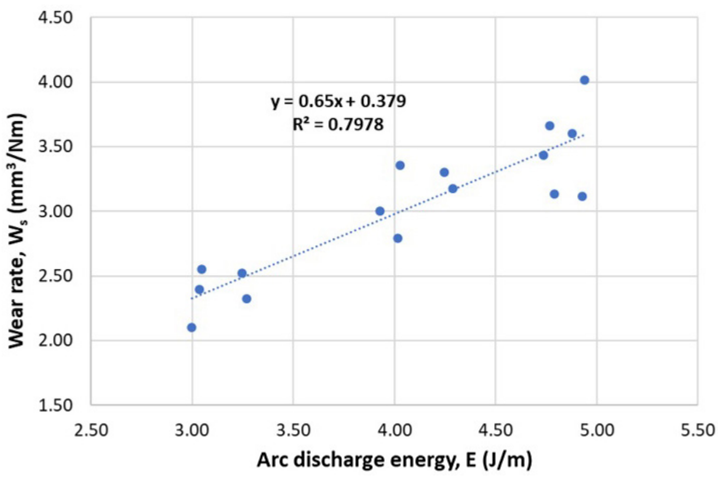

Fig. 8. Results of the orthogonal; graph based on the data [15]

arc [26]. Delamination is initiated at the edge of the large recess created by the arc, and then during the test it spreads around the recess to the entire worn surface of the carbon strip. However, the main wear mechanism found in copper contact wire is gouging and migration of copper particles. Moreover, the shape of the groove, i.e. its width and depth, changed during the test. Additionally, due to the increase in temperature at the phase boundary and the wear of the carbon tape, the migration intensity of Cu particles increases during the test.

The cumulative energy of the arc discharge E (kJ) is calculated based on the following relationship presented below [27]:

$$E = \int UIdt \quad (3)$$

where: t – time of the test, U – arc voltage,
I – current in the arc.

In the work [27] was investigated the influence of the force of dynamic contact on the arc discharges between the carbon strip and QCr0.5 chromium copper (GB/T 13808-1992) under the influence of the occurred electric current. It was found that the arcs were induced in time periods according to the period of the dynamic pressure force. These results are in opposition to previous static studies, in which arcs were always randomly generated under a constant load [28, 29]. Moreover, it was found that the number of arcing discharges increased with increasing operating speed during the test. The velocity of the arc discharges has increased from 40 km/h to 100 km/h, but a sharp increase was recorded after exceeding the velocity of 80 km/h (Fig. 10).

The obtained results of the Finite Elements Method (FEM) simulation revealed that the measured frequency and amplitude of the dynamic pressure force has increased together with the increase of the driving velocity, and allowed to include this relationship in the equation below (4):

$$F(t) = 70 + Bsin(2\pi ft) \quad (4)$$

where: B – dynamic pressure amplitude,
f – frequency.

Abrasive wear has dominated at low speeds - clear scratches and impurities in the form of scales, and the alloy copper particles were transferred to the carbon material. However, at high speeds, cracks and copper oxide particles appeared. On this basis, it was found that with increasing speed, the wear mechanism changed from friction wear to arc erosion with increasing speed.

When using direct current (DC) power supply, in the initial phase of slip, current can be transferred from the overhead line to the pantograph current collector without causing electric discharges. However, it was found that after 6–8 seconds there were two relatively large fluctuations in the electric current signals and the generated voltage, which revealed the occurrence of an electric discharge in the form of an arc. Thus, it was found that the energy of the arc discharge increases with the increase in electric current at the same sliding speed value (Fig. 11). The energy of an electric arc discharge is described as the energy of the arc discharge at the associated friction path length [30].

In the found scientific literature, it was stated that the sliding speed certainly affects the number

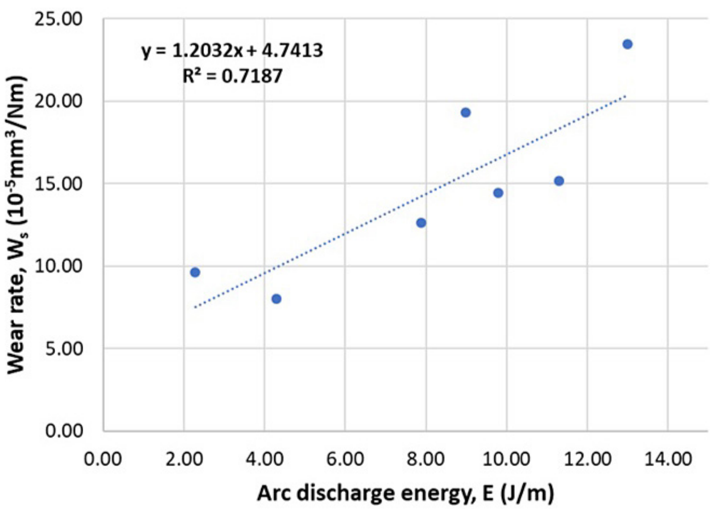

Fig. 9. Strip wear rate compared to arc discharge energy throughout the test

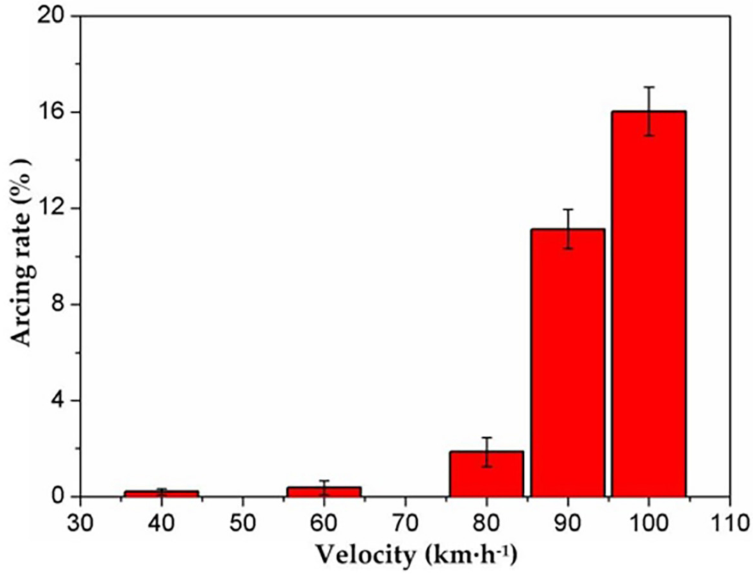

Fig. 10. Electric arc rate of the pure carbon strip in relation to the occurred velocity [27]

of discharges – the higher the speed, the greater the number of discharges in the form of an electric arc. This relationship is presented in Figure 10 and also discussed in the work [27]. It is related to the dynamic increase in the contact place of the current collector with the traction elements; generally, the higher the velocity of the train, the higher the dynamic kinetic energy which is available to the sliding guide.

The impact of slip speed on the energy of the arc discharges is shown in the Figure 11. Furthermore, in publication [31] it was found that the discharge energy E1 = 2.149e^5 for the velocity v = 150 km/h, E2 = 1.681e^5 for the velocity v = 100 km/h, and E3 = 1.225e^5 for the velocity v = 50 km/h. The ratio of arc discharge energy is equal E1/E2 = 1.30 and for E1/E3 = 1.79. However, observations show that the probability of arc occurrence decreases as the sliding velocity increases. Moreover, it can be state that the shorter the sliding speed, the shorter is the arc duration.

Another phenomenon that has a destructive effect on the guide of the section insulator may be corona discharge. It occurs when a current begins to flow in a neutral medium, usually air, from a discharge electrode connected to high voltage. Due to the ionisation of the medium, which generates plasma around the electrode, the movement of charges is possible (Fig. 12) [32]. The ions either lift the electric charge to a lower potential region that is around the collecting electrode or recombine to form neutral atoms again. If the discharge electrode has a very small radius of curvature or is a thin conductor, a large potential gradient is generated around it. A sufficiently low voltage does not allow the formation of a plasma channel, but is quite high so that the medium is partially ionised and a corona discharge is created. When the voltage in the conductor increases and the intensity of the critical field approaches about 30 kV per cm, initial discharges appear, but only on the surface of the conductor [32–34]. The necessary conditions for the formation of a corona discharge are expressed by the following equation.

$$U_0 = m_0 g_0 \delta r ln\left(\frac{s}{r}\right) \quad (5)$$

where: U_0 – discharge voltage, m_0 – cable irregularity coefficient, r – wire radius,

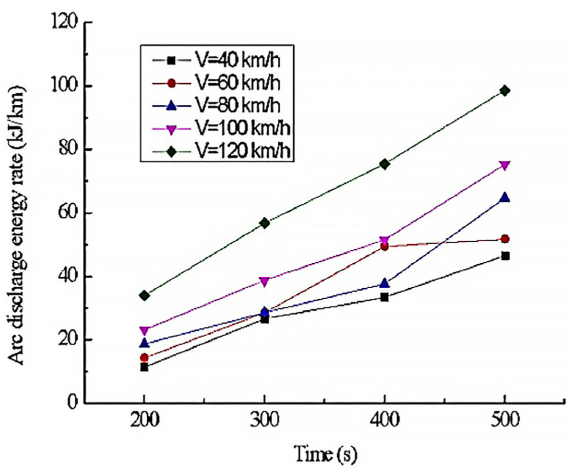

Fig. 11. Graphs of the arc discharge energy rate compared to the current [30]

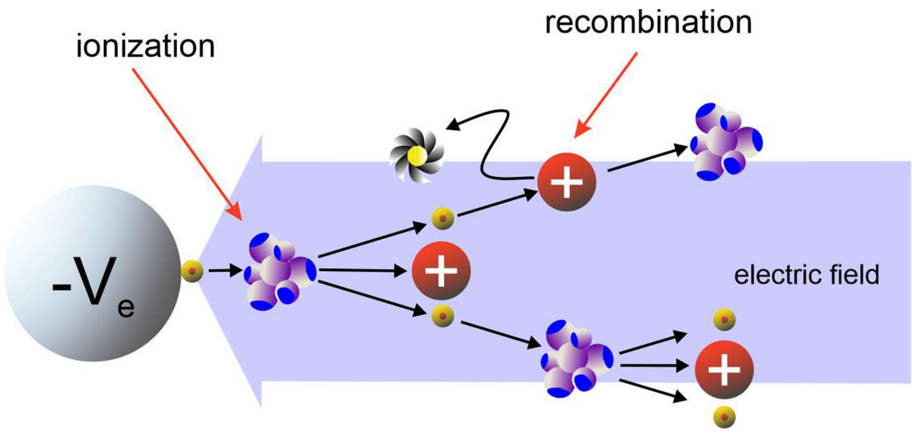

Fig. 12. The mechanism of corona discharge [33, 34]

s – distance between cables, δ – density factor, g_0 – critical potential gradient.

Corona discharges in medium- and high-voltage electrical systems are inevitable. Factors influencing the level of corona discharge include:

- atmospheric conditions: pressure, temperature and humidity;
- size and shape of the cables - the inevitable consequence of reducing the diameter of the cables, which decreases due to the action of the electric arc and wear due to friction [6]) is the formation of the crown;
- spacing between cables: the greater the distance, the less likely a corona will occur;
- the difference in potential between sections can be caused by recovering part of the braking energy of a train that was previously travelling through one of the sections.

When the passive electrode is covered with a dielectric layer of high resistivity (which in the case of rail traction may be related to, for example, floating coal dust from transported wagons) in the presence of a normal corona discharge, back-corona discharge occurs. Due to the presence of the dielectric, the ion current does not flow freely in the interelectrode area because the charge from the corona discharge causes accumulation on the dielectric surface and also causes also an increase in the strength of the electric field in the entire dielectric area as well as a decrease in the electric field strength in area between the electrodes. If the intensity of the electric field reaches a sufficient level, the dielectric layer breaks down in the form of narrow channels that reach the surface of the passive electrode. So in these craters, the ionisation of gas and dielectric material occurs [35].

CONCLUSIONS

As part of the work, analyses of damage to the delivered, worn sectional guides made of Cu-ETP copper, which were used on the overhead contact line, were performed. Microstructure studies were carried out on a micro and macro scale, as well as changes in the chemical composition in the micro-areas of damaged guides. Based on the obtained test results of the uses insulator guides, it was found the following:

1. The electric arc is the most destructive phenomenon that accompany the operation of the the guides of section insulators made of Cu-ETP copper.
2. Due to the high temperature caused by an electric arc, it is possible to melt a portion of the guide (Fig. 4), which can be very dangerous when having contact with peoples or infrastructure elements during such an electric arc discharge.
3. The consequence of induction of an electric arc is the melting of the guide surface (Fig. 6, Fig. 7a), which results in deterioration of its surface condition and promotes the induction of an electric arc during subsequent passes of the pantograph through the insulator.
4. As a result of remelting of the guide surface, particles of materials (Fig. 7b; Tab. 2) from the outside (dust cloud accompanying the train passage, transported materials, and raw materials) are feed into the material, which reduces the electrical and thermal conductivity, which increases the probability of an electric arc occurring during next train run.
5. Under favourable conditions, a corona discharge may occur, the destructive effect of

which on the guide may be comparable to the action of an electric arc.

6. Elements in the upper surface microstructure were found to come from the external environment, so efficient saving of the insulator part is suggested and required just to avoid huge electric arc discharge actions.

REFERENCES

1. Konieczny, J., Labisz, K., Adamiec, A., Młyńczak, J., Adamiak, A., Wear mechanisms of the section isolator guide. Ed. by Maciej Szkoda. Challenges for the market of production, operation and maintenance of rail vehicles. Monography. Kraków: Wydawnictwo Politechniki Krakowskiej. 2021; 236–24.
2. Wymagania dla materiałów węglowych nakładek ślizgowych pantografów dopuszczonych do współpracy z siecią trakcyjną zarządzaną przez PKP Polskie Linie Kolejowe S.A. Iet-4. [In Polish: Requirements for carbon materials of pantograph slide pads approved for cooperation with the overhead contact line managed by PKP Polskie Linie Kolejowe S.A. Iet-4]. Available at: https://www.bip.plksa.pl/files/public/user_upload/pdf/Akty_prawne_i_przepisy/Instrukcje/Wydruk/Iet/let-4_WCAG.pdf (attendance 2024.01.07)
3. Lee, S.-H., Hsu, H.-C., Tuan, W.-H., Oxidation Behavior of Copper at a Temperature below 300 °C and the Methodology for Passivation. Materials Research. 2016; 19(1): 51–56.
4. Mańka, A., Hełka, A., Ćwiek, J. Influence of Pantograph Carbon–Metal Composite Slider Thermal Properties on the Railroad Wire Temperature. Energies. 2021; 14: 7940.
5. Wu, G., Wu, J., Wei, W., Zhou, Y., Yang, Z., Gao, G. Characteristics of the Sliding Electric Contact of Pantograph/Contact Wire Systems in Electric Railways. Energies. 2018; 11: 17.
6. Konieczny, J. Destruction mechanisms of Cu-ETP copper guides for sectional insulators of railway traction. Scientific Journal of the Silesian University of Technology. Series Transport. 2021; 113: 101-113.
7. Kano, R., Nemoto, Y., Maeda, Y., Yamamoto, S., Iwao, T. Arc temperature measurement with microsecond spectroscopic measurement. Electrical Engineering in Japan. 2019; 139(10): 629–635.
8. Csanyi, E. Consequences of internal arc for personal safety and MV electric equipment. Electrical Engineering Portal. 2011. Available at: https://electrical-engineering-portal.com/consequences-of-internal-arc-for-personal-safety-and-mv-electrical-equipment (attendance 2024.01.07)
9. Armijo, K.M., Clem, P.G., Kotovsky, D., Demosthenous, B., Tanbakuchi, A., Martinez, R.J., Muna, A.B., LaFleur, C.B. Electrical Arc Fault Particle Size. Characterization. Sandia National Laboratories, United States Department of Energy by National Technology & Engineering Solutions of Sandia, LLC. 2019.
10. Das, J.C. Arc Flash Hazard Analysis and Mitigation. John Wiley & Sons. 2012; Edition 1.
11. BN-769317-109. Sieć trakcyjna kolejowa. Izolatory sekcyjne. Warszawa: Centralny Ośrodek Badań i Rozwoju Techniki Kolejnictwa/Instytut Kolejnictwa. [In Polish: BN-769317-109. Railway traction network. Section insulators. Warsaw: Central Research and Development Center of Railway Technology/Railway Research Institute].
12. PN-EN 1976:2013-04. Miedź i stopy miedzi. Wyroby odlewane z miedzi nieprzerobione plastycznie. Warszawa: Polski Komitet Normalizacyjny. [In Polish: PN-EN 1976:2013- 04. Copper and copper alloys. Copper-cast products not wrought. Warsaw: Polish Committee of Standardization].
13. PN-EN 1652:1999. Miedź i stopy miedzi. Płyty, blachy, taśmy i krążki ogólnego przeznaczenia. Warszawa: Polski Komitet Normalizacyjny. [In Polish: PN-EN 1652:1999. Copper and copper alloys. General-purpose plates, sheets, strips and pulleys. Warsaw: Polish Committee of Standardization].
14. Wu, G., Gao, G., Wei, W., Yang, Z. The Electrical Contact of the Pantograph-Catenary System Theory and application. Springer Nature Singapore Pte Ltd. 2019.
15. Hu, D.-Ch., Wang, L., Sun, L-M., Effects of arc discharge on wear properties of carbon-carbon composites sliding against Cu trolley under electric current. Materials Science Forum. 2011; 675–677: 407–410.
16. Jüttner, B. Cathode spot of electric arc. Journal of Physics D: Applied Physics. 2001; 34: 103–123.
17. Anders, A. Cathodic Arcs: From Fractal Spots to Energetic Condensation. Springer New York, NY. 2008
18. Langley, R.A. Data compendium for plasma-surface interactions. Nuclear Fusion. New York. 1984; 24: 001.
19. Daadler, J.E. Cathode spots and vacuum arcs. Physica B+C. 1981; 104(1–2): 91–106.
20. Rohde, V., Balden, M. Arc erosion of full metal plasma facing components at the inner baffle region of ASDEX Upgrade. Nuclear Materials and Energy. 2016; 9: 36–39.
21. Yang, H.J., Chen, G.X., Zhang, S.D., Zhang, W.H. Effect of the vibration on friction and wear behavior between the carbon strip and copper contact wire pair. Proc I Mech E Part J: J Engineering Tribology. 2012; 226(8): 722–728.
22. Lin, X.-Z., Zhu, M.-H., Mo, J.-L., Chen G.-X., Jin, X.-S., Zhou, Z.-R. Tribological and electric-arc behaviors of carbon/copper pair during sliding friction process with electric current applied. Trans.

Nonferrous Met. Soc. China. 2011; 21: 292–299.

23. Kubo, S., Kato, K. Effect of arc discharge on wear rate of Cu-impregnated carbon strip in unlubricated sliding against Cu trolley under electric current, Wear. 1998; 216: 172–178.
24. Kubo, S., Kato, K. Effect of arc discharge on the wear rate and wear mode transition of a copper-impregnated metallized carbon contact strip sliding against a copper disk, Tribology International. 1999; 32: 367–378.
25. Ding, T., Chen, G-X., Li, Y-M., He, Q-F., Xuan, W-J. Fricton and wear behaviour of pantographs strip sliding against copper contact wire with electric current. AASRI Conference for Power and Energy System. AASRI Procedia. 2012; 2: 288–292.
26. Yang, H., Wang, K., Liu, Y., Fu, L., Cui, X., Jiang, G., Hu, B. The formation of the delamination wear of the pure carbon strip and its influence on the friction and wear properties of the pantograph and catenary system. Wear. 2020; 454–455: 203343.
27. Zhang, Y.Y., Zhang, Y.Z., Song, C.F. Arc discharges of a pure carbon strip affected by dynamic contact force during current-carrying sliding. Materials. 2018; 11(5): 796–810.
28. Chen, G.X., Yang, H.J., Zhang, W.H., Zhang, X., Wang, S.D. Experimental study on arc ablation occurring in a contact strip rubbing against a contact wire with electrical current. Tribology International. 2013; 61: 88–94.
29. Yang, Z.H., Zhang, Y.Z., Zhao, F., Shangguan, B. Dynamic variation of arc discharge during current-carrying sliding and its effect on directional erosion. Tribology International. 2016. 94: 71–76.
30. Mei, G. Tribological performance of rigid overhead lines against pantograph sliders under DC passage. Tribology International. 2020; 151: 106538.
31. Chen, G.X., Hu, Y., Dong, B.J., Yang, H.J., Gao, G.Q., Wu G.N., Zhang, W.H., Zhou, Z.R. Experimental study on the temperature of the contact strip in sliding electric contact, Proceedings of the Institution of Mechanical Engineers Part J Journal of Engineering Tribology. 2017; 208–210; 1994–1996.
32. Durak, S., Partyka, J., Gustaw, M. Measurements and analysis of partial discharges using a corona discharge camera. Electrotechnical Review. 2020; 96(8): 156–159. (in Polish)
33. Florkowska, B., Furgał, J. High voltage technique. Theoretical basis and laboratory. Wydawnictwo AGH. 2017. Kraków. (in Polish)
34. Grill, P. Electrical Power Equipment Maintenance and Testing. Second Edition. CRC Press. 2009.
35. Jaworek, A., Czech, T., Krupa, A., Lackowski, M., Rajch, E. Back discharge morphology. In: 6th Scientific and Technical Conference of Electrofilters. 2002. Cracow. September 19–21, 2002.
36. Piec, M., Dobrzański, L.A., Labisz, K., Jonda, E., Klimpel, A. Laser alloying with WC Ceramic Powder in hot work tool steel using a High Power Diode Laser (HPDL), Advanced Materials Research 2007; 15–17: 193–198.
37. Stańczyk, M., Figlus, T. The influence of the hardening coolant agent on the properties of hot rolled bars of the steel 42CrMo4, Metalurgija, 2014; 53(4): 493–493.